J Appl Electrochem
DOI 10.1007/s10800-010-0188-5

ORIGINAL PAPER

Green synthesized Au–Ag bimetallic nanoparticles modified electrodes for the amperometric detection of hydrogen peroxide

Tsung-Hsuan Tsai · Soundappan Thiagarajan · Shen-Ming Chen

Received: 3 February 2010 / Accepted: 5 September 2010

Abstract Simple and eco-friendly electro deposition method was employed for the fabrication of Au–Ag bimetallic nanoparticles modified glassy carbon electrode. Nano Au–Ag film modified glassy carbon electrode surface morphology has been examined using atomic force microscopy. Electrodeposited Au–Ag bimetallic nanoparticles were found in the average size range of 15–50 nm. The electrochemical investigations of nano Au–Ag/1-butyl-3-methylimidazolium tetrafluoroborate-nafion film have been carried out using cyclic voltammetry and electrochemical impedance spectroscopy. The nano Au–Ag/1-butyl-3-methylimidazolium tetrafluoroborate-nafion film modified glassy carbon electrode holds the good electrochemical behavior and stability in pH 7.0 phosphate buffer solutions. The nano Au–Ag/1-butyl-3-methylimidazolium tetrafluoroborate-nafion modified glassy carbon electrode was successfully employed for the detection of H_2O_2 in the linear range of 1–250 μM in lab samples, and 1×10^{-3}–2×10^{-2} M in real samples, respectively.

Keywords Au–Ag bimetallic nanoparticles · Ionic liquid · Cyclic voltammetry · Amperometry · H_2O_2

1 Introduction

The detection and determination of hydrogen peroxide (H_2O_2) was found as important dispute in the field of biosensor research. Previously, various methods such like spectrometry [1], chemiluminescence [2], flame absorption spectrometry [3] and titrimetry have been utilized for the detection of H_2O_2. Comparing with these methods, electrochemical method [4–8] is found to be effective for the detection and determination of H_2O_2. Hence, here we focused to develop a nanomaterials modified electrodes for the detection of H_2O_2. Room temperature ionic liquids (RTILs) have been found as interesting green electrolytes for the fabrication of nanomaterials. Especially, RTILs are suitable medium for the fabrication of catalytically active transition metal nanoparticles. Also, RTILs could be functionalized for their enhanced catalytic activity and recyclability [9].

Therefore, utilizing ionic liquids as green electrolytes for the fabrication of nanomaterials have been found as new topic for the design and development of future biosensors. Further different type of nanomaterials modified electrodes have been reported for the fabrication of H_2O_2 sensor. For example, nano Au based H_2O_2 sensors were, nano Au matrix modified ITO [10, 11], Au in chitosan matrix [12], multiwall carbon nanotubes and Au colloidal nanoparticles [13], Au nanoparticles embedded in silica sol–gel matrix [14], Au colloid/L-cysteine/Au colloid/nanoparticles Pt–chitosan composite film [15], AuNPs–C@SiO_2 composite [16], ZnO–Au nanoparticle–nafion nanocomposite [17] and metal nanoparticles modified screen printed carbon electrodes (SPCE) [18]. Ag nanoparticles based sensors were; Ag nanoparticles electrodeposited on DNA-networks modified glassy carbon electrode (GCE) [4], DNA–Ag nanohybrids [19], Ag nanoparticles on a type I collagen-modified GCE [20] and Ag microspheres [21]. Further in bimetallic particles, ultrasonic electrodeposition of gold–platinum alloy nanoparticles on ionic liquid-chitosan composite film [22] for H_2O_2 detection also accounted.

T.-H. Tsai · S. Thiagarajan · S.-M. Chen (✉)
Electroanalysis and Bioelectrochemistry Lab, Department of Chemical Engineering and Biotechnology, National Taipei University of Technology, No. 1, Section 3, Chung-Hsiao East Road, Taipei 106, Taiwan, ROC
e-mail: smchen78@ms15.hinet.net

Published online: 18 September 2010

This report has been particularly focused to develop a method for the one step electrochemical deposition of Au–Ag bimetallic nanoparticles using ionic liquid as green electrolyte. Here the GCE has been utilized for the fabrication of Au–Ag bimetallic nanoparticles. The Au–Ag bimetallic nanoparticles modified film has been characterized using atomic force microscopy (AFM). The proposed film modified GCE was employed for the amperometric detection of H_2O_2. The Au–Ag bimetallic nanoparticles modified GCE showed linear response for the detection of H_2O_2 in lab and real samples.

2 Materials and methods

2.1 Chemicals and reagents

1-Butyl-3-methylimidazolium tetrafluoroborate (BMT) (purum > 97%, HPLC), silver per chlorate, anhydrous, 97% and Nafion (per fluorinated ion exchange resin, 5% weight solution in lower aliphatic alcohols/H_2O mix (contains 15–20% water)) were purchased from Sigma-Aldrich (USA). $KAuCl_4{\cdot}3H_2O$ was purchased from Strem Chemicals (USA). All other chemicals (Merck) used were of analytical grade (99%). Double distilled deionized water was used to prepare all the solutions. A phosphate buffer solution (PBS) of pH 7.0 was prepared using Na_2HPO_4 (0.05 mol L^{-1}) and NaH_2PO_4 (0.05 mol L^{-1}). Pure nitrogen was passed through all the experimental solutions.

2.2 Apparatus

Cyclic voltammetry (CV) was performed using CHI 1205a potentiostats (CH Instruments, USA). The BAS glassy carbon electrode (GCE) ($\varphi = 0.3$ cm in diameter, exposed geometric surface area 0.07 cm^2, Bioanalytical Systems, Inc., USA) was used. A conventional three-electrode system was used which consists of an Ag/AgCl (saturated KCl) as a reference, bare or nano Au–Ag/BMT-Nf modified GCE as working and platinum wire as counter electrode. For nano Au–Ag film deposition process ionic liquid filled (BMT) Ag electrode (Ag/ionic liquid) has been used as the reference. For the rest of the electrochemical studies Ag/AgCl (saturated KCl) was used as a reference. Electrochemical impedance studies (EIS) were obtained using ZAHNER impedance analyzer (Germany). The AFM studies were performed using a multimode scanning probe microscope (Being Nano-Instruments CSPM-4000, China).

2.3 Fabrication of Au–Ag bimetallic nanoparticles

The Au–Ag bimetallic nanoparticles have been fabricated based on previous literature report (immersing the pretreated GCE in 1 mL 1-butyl-3-methylimidazolium tetrafluoro borate containing 1 mM $KAuCl_4{\cdot}3H_2O$ and $AgClO_4$. CV was employed for the electrochemical deposition process. The Au–Ag bimetallic nanoparticles have been directly deposited on GCE surface by applying a repetitive potential scan between 1.0 and −1.0 V (vs. Ag/ionic liquid) at the scan rate of 0.05 V s^{-1} for five cycles) [23]. Further the Au–Ag bimetallic nanoparticles modified GCE was washed with deionized water and dried for 5 min. To prevent the easy oxidation, the Au–Ag bimetallic nanoparticles modified GCE surface was further coated with 4 μL of nafion and ionic liquid (BMT) mixture (ratio (1:1)) and dried in air and kept in refrigerator for 2 h at 4 °C. Hereafter the film modified GCE was denoted as nano Au–Ag/BMT-Nf film modified GCE.

3 Results and discussion

3.1 Characterization of nano Au–Ag/BMT-NF film

The nano Au–Ag/BMT-NF film modified GCE was employed for the different scan rate studies. Figure 1 shows the cyclic voltammograms of nano Au–Ag/BMT-Nf film modified GCE in pH 7.0 PBS. Here the Au reduction peak at the lower scan rate appears at 0.51 V and for the increasing scan rates it shifts to negative potentials and for 1 V s^{-1} it appears at 0.43 V. At the same time, the Au oxidation peak initially appears at 0.91 V, at the higher scan rate it appears at 0.95 V. In Ag case, the reduction peak appears at 0.11 V and shifts to the negative potential, at the higher scan rate it appears at 0.09 V. Further the oxidation peak of Ag appears at 0.30 V and shifts to positive potential and finally appears at 0.34 V for 1 V s^{-1}. Here all the anodic and cathodic peak currents of Au–Ag increases linearly with respect to the scan rate in the range of 0.01–1 V s^{-1}. At the same time, the anodic and cathodic peak currents of Au appears higher than the Ag. This is because of the easy oxidation nature of Ag. Further the insets of Fig. 1 show the plot of anodic and cathodic peak current versus scan rate of Au and Ag. Finally, the linear increase in the anodic and cathodic peak currents of nano Au–Ag/BMT-Nf film according to the scan rate illustrates that the proposed film was stable and exhibits the surface controlled thin-layer electrochemical behavior, respectively.

3.2 AFM and EIS analysis

Surface morphology of the Au–Ag bimetallic nanoparticles modified GCE has been examined using AFM technique. Here the tapping mode was utilized for the surface analysis. The AFM parameters have been evaluated for 1375 × 1378 nm surface area. Figure 2a shows the 2D view of the

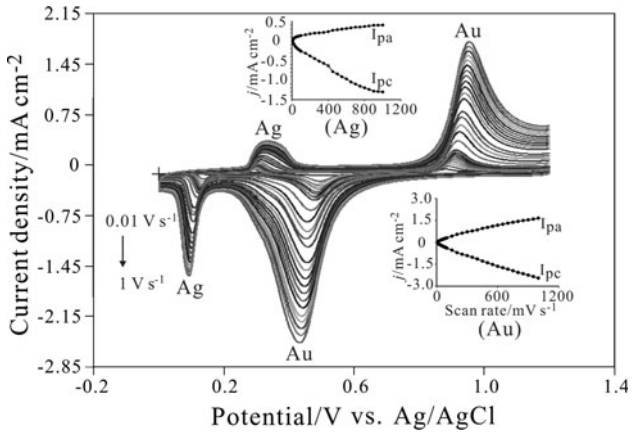

Fig. 1 CVs of nano Au–Ag/BMT-Nf film modified GCE. Scan rate in the range of 0.01–1 V s^{-1}. *Inset* shows the plot of anodic and cathodic peak current versus scan rate of the electrodeposited Au–Ag on GCE (in pH 7.0 PBS)

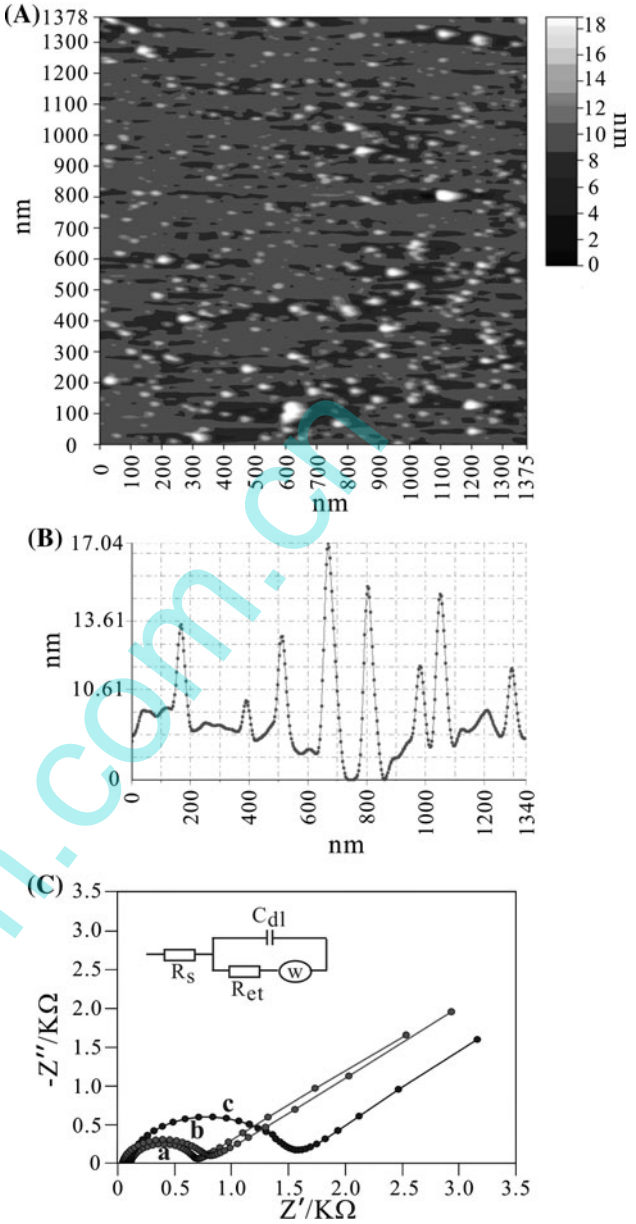

Fig. 2 Tapping mode AFM image of Au–Ag bimetallic nanoparticles modified GCE. **a** Topographic (2D) view of Au–Ag bimetallic nano film on GCE. **b** Cross-sectional analysis graph and **c** Electrochemical impedance spectra curves of (*a*) bare GCE (*b*) Au–Ag bimetallic film and (*c*) nano Au–Ag/BMT-Nf film modified GCE in pH 7.0 PBS containing 5 × 10^{-3} M $[Fe(CN)_6]^{3-/4-}$ (Amplitude: 5 mV)

Au–Ag bimetallic nanoparticles modified GCE. Figure 2b shows the cross-sectional analysis graph of the Au–Ag bimetallic nanoparticles electrodeposited GCE. Based on this analysis, the Au–Ag bimetallic nanoparticles were found in the average size range of 15–50 nm. The other amplitude parameters such like the roughness average (sa) (1375 × 1378 nm) was found as 1.08 nm. The skewness (Rsk) measures the symmetry variation of the surface about its mean plane. Here the positive skewness value (1.85) obtained shows that the surface comprised of disproportionate peaks which indicate that the nano Au–Ag particles were unevenly electrodeposited on the GCE surface. Next, the kurtosis (Rku) is a measure of the unevenness or sharpness of the surface. A surface that is centrally distributed has a kurtosis value greater than three. For Au–Ag bimetallic nanoparticles film, the kurtosis value was found as 9.52. Further based on the height normal distribution the average height of Au–Ag bimetallic nanoparticles film was found as 3.24 nm. In particular, the maximum numbers of Au–Ag bimetallic nanoparticles have been found in the size range of 18 nm. Here the total number of Au–Ag bimetallic nanoparticles found for the 1375 × 1378 nm surface area was 851, respectively. Finally the above AFM results clearly illustrate the surface nature of the Au–Ag bimetallic nanoparticles modified GCE.

The electrochemical activity of nano Au–Ag bimetallic/BMT-Nf modified GCE has been examined using EIS technique. The electron-transfer kinetics and diffusion characteristics could be clearly analyzed using the EIS analysis. Here the complex impedance presented as a sum of the real, Z′ (ω), and imaginary Z″ (ω), components that originate mainly from the resistance and capacitance of the cell. Figure 2c represents the Faradaic impedance spectra, presented as Nyquist plots (Z″ vs. Z′) for the Au–Ag bimetallic film, nano Au–Ag/BMT-Nf film modified GCE and bare GCE, respectively. Here the bare GCE Fig. 2c curve a exhibits as very small depressed semi circle arc (R_{et} = 0.68 (Z′/KΩ)) represents the characteristics of diffusion limited electron-transfer process on the electrode surface. Further Au–Ag bimetallic nanoparticles modified GCE (curve b) exhibits as like a distinguished semi-circular arc with larger electron transfer resistance value (R_{et} = 0.81 (Z′/KΩ)). At the same time, the nano Au–Ag/BMT-Nf film modified GCE (curve c) exhibits as a big

semi-circular arc with higher electron transfer resistance (R_{et} = 1.53 (Z′/KΩ)) comparing with curve a and curve b. This is because the additional coatings of BMT-NF on the Au–Ag bimetallic nanoparticles film modified GCE, respectively. Finally, the EIS analysis results clearly illustrate the electrochemical activities of the nano Au–Ag, nano Au–Ag/BMT-Nf film modified GCE.

3.3 Detection of H_2O_2 at nano Au–Ag/BMT-Nf film modified GCE

Electrocatalytic response of nano Au–Ag/BMT-Nf film (curve b) has been compared with Ag nanoparticles (curve c), Au nanoparticles modified GCE (curve d) and bare GCE (curve a′) (Fig. 3). Here curve a shows the CV response of nano Au–Ag/BMT-Nf film modified GCE in pH 7.0 PBS (absence of H_2O_2). For the 1.7×10^{-3} M concentration range, in pH 7.0 PBS, the nano Au–Ag/BMT-Nf film modified GCE (curve b) exhibits the H_2O_2 reduction signal around −0.4 V. At the same time, the only Ag and Au modified GCEs also show the current response for H_2O_2 reduction at −0.4 V. However, comparing with the nano Au–Ag/BMT-Nf film, the only Ag and only Au nanoparticles modified GCE's current response for the H_2O_2 reduction were too low. This shows that the presence of both Au–Ag nanoparticles possess the higher electrocatalytic activity comparing with the only Au or Ag nanoparticles. Here both the nano Au and Ag particles exhibit their own electrocatalytic activity. Therefore, we could also notice the individual oxidation peaks in the reverse cycle, respectively. At the same time, at the bare GCE (curve a′), there is no significant response for the electrochemical reduction of H_2O_2. Therefore, increase in the reduction peak current and decrease in the over potential at nano Au–Ag/BMT-Nf film modified GCE show that the proposed film successfully reduces the H_2O_2. Next the nano Au–Ag/BMT-Nf modified GCE was employed for the amperometric detection of H_2O_2.

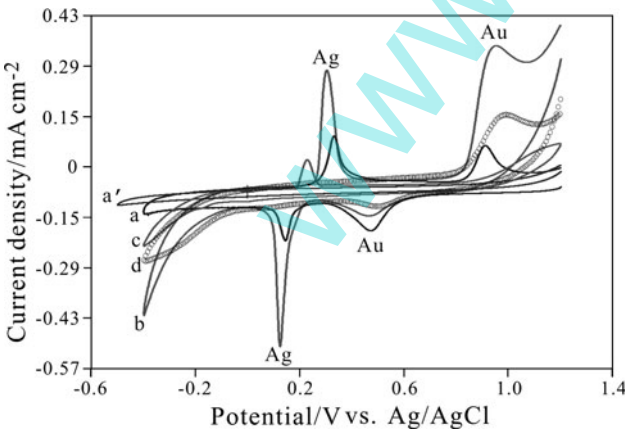

Fig. 3 (*a*) CV response of nano Au–Ag/BMT-Nf modified GCE in pH 7.0 PBS (absence of H_2O_2), (*b*) CV response of nano Au–Ag/BMT-Nf modified GCE in pH 7.0 PBS containing 7×10^{-3} M H_2O_2, (*c*) Ag modified GCE, (*d*) Au modified GCE and (*a′*) bare GCE for 7×10^{-3} M H_2O_2 in pH 7.0 PBS

Figure 4a shows the amperometric response of nano Au–Ag/BMT-Nf film modified GCE in pH 7.0 PBS for the different concentrations of H_2O_2. Here nano Au–Ag/BMT-Nf film modified GCE showed the amperometric current response for H_2O_2 reduction within the 5 s. Also, for the increasing additions of H_2O_2, the reduction current was clearly increasing up to the value of 250 μM. From the calibration plot (Fig. 4a), the linear regression equation for the H_2O_2 reduction at the nano Au–Ag/BMT-Nf film modified GCE was expressed as $I_{pc} = 0.052$ C (μM) + 19.24, $R^2 = 0.964$. From this result, the electrocatalytic activity of the proposed nano Au–Ag/BMT-Nf film modified GCE for H_2O_2 reduction has been validated.

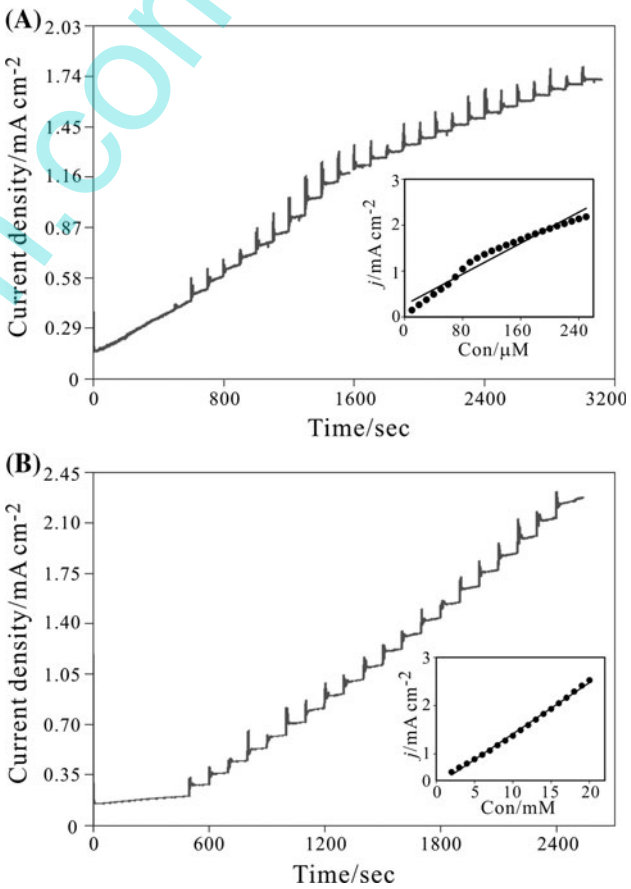

Fig. 4 **a** Amperometric i–t response of the nano Au–Ag/BMT-Nf film modified GCE in pH 7.0 PBS for the sequential additions of H_2O_2 (1–250 μM, potential: −0.4 V). The *inset* shows the current versus concentration plot for the H_2O_2 detection. **b** Amperometric i–t response of the nano Au–Ag/BMT-Nf film modified GCE in pH 7.0 PBS for the sequential additions of antiseptic solution containing (30% H_2O_2) (1×10^{-3}–2×10^{-2} M, potential: −0.4 V). The *inset* shows the current versus concentration plot for the H_2O_2 detection

In the next attempt, the nano Au–Ag/BMT-Nf film modified GCE was directly employed for the detection of H_2O_2 in real samples (Fig. 4b). For the real sample analysis, commercially available antiseptic solution (containing 30% H_2O_2) was examined. Here also the proposed nano Au–Ag/BMT-Nf film successfully shows the amperometric current response for the detection of H_2O_2 in higher concentrations ranges. As expected, the nano Au–Ag/BMT-Nf film modified GCE shows the amperometric current response for the H_2O_2 detection within 5 s following with the additions of the antiseptic solution in pH 7.0 PBS. The linear regression equation for the H_2O_2 detection in the real sample at the nano Au–Ag/BMT-Nf film was $I_{pc} = 4.146\ C\ (mM) + 15.24$, with the correlation coefficient of $R^2 = 0.996$. Finally, these results clearly show that the nano Au–Ag/BMT-Nf film modified GCE holds the capacity for the detection and determination of H_2O_2 in the lab and real samples.

3.4 Interference and stability studies

The selectivity of nano Au–Ag/BMT-Nf film modified GCE for the H_2O_2 detection has been evaluated with five species (ascorbic acid (AA), uric acid (UA), L-cysteine (LC), glucose, dopamine (DA), L-tyrosine (LT) (5×10^{-4} M) (H_2O_2 concentration 1×10^{-3} M)). No obvious current response was observed for the injection of these compounds (AA, UA, LC, glucose, DA, L-tyrosine) (Fig. 5). This suggests that nano Au–Ag/BMT-Nf film modified GCE selectively detects the H_2O_2 in the presence of these interferences, respectively. Further the stability of the nano Au–Ag/BMT-Nf film modified GCE was investigated by storing it in pH 7.0 PBS at 4 °C (Fig. 6). It was stable for 1 week and after that gradual decrease occurred in its reduction peak currents (Ag (13%) and Au (14%)). This result shows that the nano Au–Ag/BMT-Nf film holds the sufficient stability in the specific conditions, respectively.

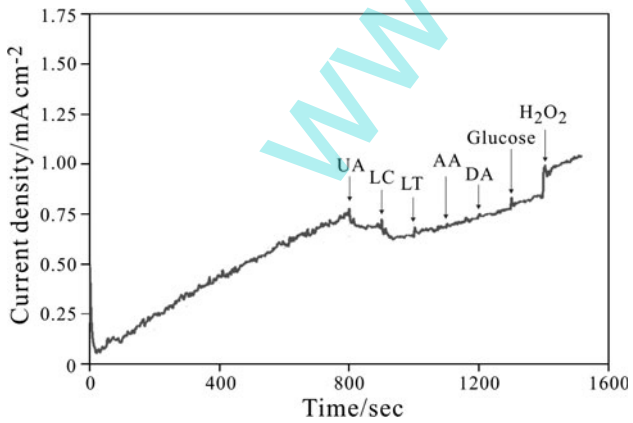

Fig. 5 Amperometric i–t response of the nano Au–Ag/BMT-Nf film modified GCE for the sequential additions of UA, LC, LT, AA, DA, glucose and H_2O_2 (pH 7.0 PBS)

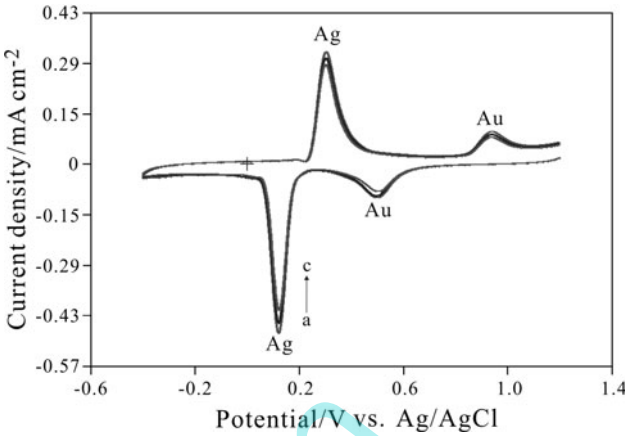

Fig. 6 CV response of nano Au–Ag/BMT-Nf film modified GCE in the pH 7.0 PBS: (*a*) first day, (*b*) after 3 days and (*c*) after 7 days

4 Conclusion

In conclusion, we have successfully employed one step electrochemical deposition method using ionic liquid as green electrolyte for the fabrication of nano Au–Ag/BMT-Nf film modified GCE. Fabricated nano Au–Ag/BMT-Nf film modified GCE has been characterized using CV, AFM and EIS analysis. The nano Au–Ag/BMT-Nf film modified GCE effectively showed the current response for the detection of H_2O_2 within the applicable concentration range in the lab and real samples. Also, the nano Au–Ag/BMT-Nf film modified GCE could be employed for the other type of electrochemical and biosensing applications.

Acknowledgment This work was supported by National Science Council (NSC) of Taiwan (ROC).

References

1. Hurdis EC, Romeyn H (1954) Anal Chem 26:320
2. Matsubara C, Kawamoto N, Takamura K (1992) Analyst 117:1781
3. Nakashima K, Maki K, Kawaguchi S, Akiyama S, Tsukamoto Y, Imai K (1991) Anal Sci 7:709
4. Cui K, Song Y, Yao Y, Huang ZZ, Wang L (2008) Electrochem Commun 10:663
5. Golabi SM, Raoof JB (1996) J Electroanal Chem 416:75
6. Song Y, Wang L, Ren C, Zhu G, Li Z (2006) Sens Actuators B Chem 114:1001
7. Lian W, Wang L, Song Y, Yuan H, Zhao S, Li P, Chen L (2009) Electrochim Acta 54:4334
8. Tânia M, Benedetti TM, Bazito FFC, Ponzio EA, Torresi RM (2008) Langmuir 24:3602
9. Zhao D, Fei Z, Geldbach TJ, Scopelliti R, Dyson PJ (2004) J Am Chem Soc 126:15876

10. Zhang J, Oyama M (2004) Electrochim Acta 50:85
11. Zhang J, Oyama M (2005) J Electroanal Chem 577:273
12. Tangkuaram T, Ponchio C, Kangkasomboon T, Katikawong P, Veerasa W (2007) Biosens and Bioelectron 22:2071
13. Chen S, Yuan R, Chai Y, Zhang L, Wang N, Li X (2007) Biosens and Bioelectron 22:1268
14. Maduraiveeran G, Ramaraj R (2007) J Electroanal Chem 608:52
15. Yang G, Yuan R, Chai YQ (2008) Coll Surf B Biointerface 61:93
16. Wang Y, Chen X, Zhu JJ (2009) Electrochem Commun 11:323
17. Xiang C, Zou Y, Sun LX, Xu F (2009) Sens Actuat B 136:158
18. Chikae M, Idegami K, Kerman K, Nagatani N, Ishikawa M, Takamura Y, Tamiya E (2006) Electrochem Commun 8:1375
19. Ma L, Yuan R, Chai Y, Chen S (2009) J Mol Catal B Enzym 56:215
20. Song Y, Cui K, Wang L, Chen S (2009) Nanotech 20:105501
21. Zhao B, Liu Z, Liu G, Li Z, Wang J, Dong X (2009) Electrochem Commun 11:1707
22. Xiao F, Zhao F, Zhang Y, Guo G, Zeng B (2009) J Phys Chem C 113:849
23. Tsai TH, Thiagarajan S, Chen SM (2010) J Appl Electrochem 40:493